Organic & Biomolecular Chemistry

PAPER

View Article Online
View Journal

Cite this: DOI: 10.1039/c4ob01842g

Rapid detection of hydrazine in a naphthol-fused chromenyl loop and its effectiveness in human lung cancer cells: tuning remarkable selectivity *via* the reaction altered pathway supported by theoretical studies†

Shyamaprosad Goswami,*[a] Avijit Kumar Das,[a] Urmila Saha,[b] Sibaprasad Maity,[a,c] Kalyani Khanra[d] and Nandan Bhattacharyya[d]

Received 29th August 2014,
Accepted 5th December 2014

DOI: 10.1039/c4ob01842g

www.rsc.org/obc

Our designed and synthesized chemosensor naphthalene based chromenyl derivative (NAC) [1-(3-hydroxy-3 methyl-3*H*-benzo[*f*]chromen-2-yl) ethanone] has been used for fast (<30 s, DL = 0.22 ppb) and selective detection of N_2H_4 by a new way *via* the chromenyl ring opening followed by the pyrazole ring formation giving a strong blue fluorescence. The DFT study and the real application in different water samples along with the dipstick method in low cost devices have also been performed here. Human lung cancer cells (NCI-H460) have been used for hydrazinolysis of the NAC *in vivo* system for detection by the appearance of blue fluorescence and also for the MTT assay showing its remarkable cancer sensitivity.

To explore the proficient and selective signaling and imaging systems for the detection of various chemically and biologically relevant species is a significant area for supramolecular research.[1] Different sophisticated systems based on optically responsive molecular frameworks have been designed and synthesized for the selective and sensitive detection of various target species by different pathways (*e.g.* hydrogen bonding interaction, chemodosimetric approach *etc.*).[2] Among the different signaling pathways, an interesting and attractive strategy is to use different analyte-triggered selective transformation of latent derivatives of different fluorophores to yield signaling fluorochromes.[3–5] The technique of derivatisation of the signaling fluorophore by masking the signaling unit and the analyte-mediated conversion to different derivatives containing the parent fluorophore by demasking the signaling unit creates a fantastic policy in the organic sensing field. Furthermore among these analytes, hydrazine plays a prominent role in this type of recognition phenomenon. Thus, the selective and sensitive fluorometric detection of trace hydrazine has gained increasing attention in recent years.[6]

A highly reactive base and reducing agent, hydrazine (N_2H_4) plays vital roles in the pharmaceutical, chemical and agricultural industries, textile dyes, corrosion inhibitors, and pharmaceutical intermediates, and it is also known as a high-energy rocket-fuel in propulsion and missile systems for its detonable characteristics.[7] However, due to the toxic effects, hydrazine can lead to serious ecological contamination during its manufacture, transport, utilisation and disposal. Exposure to hydrazine at high levels (10 ppb, threshold limit by U.S. Environmental Protection Agency (EPA)) can cause irritation of the nose, blindness, pulmonary edema and damage of DNA and even the central nervous system.[8] Hydrazine also has a mutagenic and carcinogenic effect which causes severe harm to the liver, kidneys and lungs.[9] To date there are only a few reports on different phenomena for hydrazine detection *e.g.* polymer reduction by hydrazine vapour,[10] deprotection of levulinoyl or acetyl ester,[11] ratiometric response to hydrazine with arylidenemalononitrile,[12] and hydrazine reaction with aryl aldehyde.[13] But apart from these, our designed and synthesized naphthalene (having a short fluorescence lifetime, low fluorescence quantum yield and ability to act as a donor as well as an acceptor)[14] based chromenyl derivative [1-(3-hydroxy-3 methyl-3*H*-benzo[*f*]chromen-2-yl)ethanone] (**NAC**) senses hydrazine on a quite different and a new chemodosimetric approach by the

[a]*Department of Chemistry, Indian Institute of Engineering Science and Technology, Shibpur, West Bengal, India. E-mail: spgoswamical@yahoo.com*
[b]*Jadavpur University, Jadavpur, Kolkata, West Bengal, India*
[c]*Department of Applied Sciences, Haldia Institute of Technology, Hatiberia, Haldia, West Bengal-721657, India*
[d]*Panskura Banamali College, Panskura, India*
† Electronic supplementary information (ESI) available. See DOI: 10.1039/c4ob01842g

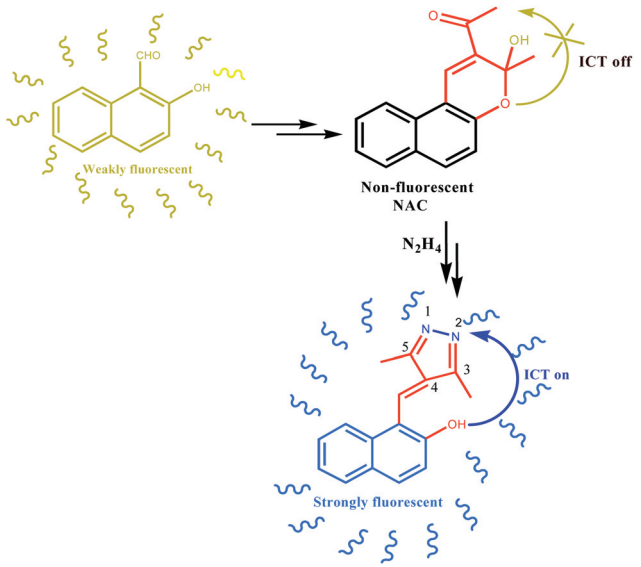

Scheme 1 The transformation of weakly fluorescent 2-hydroxy-1-naphthaldehyde to the non-fluorescent probe **NAC** and the hydrazine mediated conversion of NAC to strongly fluorescent 3,5-dimethyl-4-methylene-4*H*-pyrazole containing a chromenyl derivative (**NAP**).

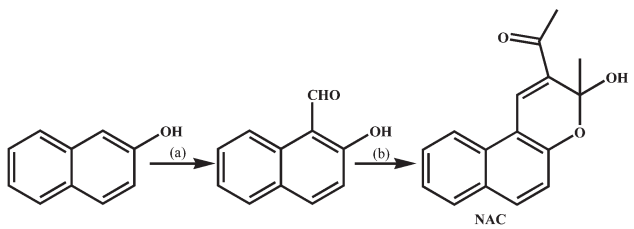

Scheme 2 (a) $CHCl_3$, NaOH, EtOH, 6 h. (b) Piperidine, dry EtOH, acetylacetone, rt, 2 h.

masking–demasking pathway of a signaling unit (naphthyl-OH) in the parent fluorophore (Scheme 1).

The synthesis of **NAC** is shown in Scheme 2. The intermediate 2-hydroxy-1-naphthaldehyde was prepared *via* Reimer–Tiemann formylation of 2-naphthol and the target compound **NAC** was prepared by the piperidine base catalysed condensation reaction between 2-hydroxy-1-naphthaldehyde in dry EtOH. The products were well characterized by ^{1}H NMR, ^{13}C NMR, and HRMS spectroscopy.

Results and discussion

The optical responses of **NAC** to N_2H_4 were exemplified through its reaction with hydrazine in CH_3CN–HEPES buffer (50/50, v/v, pH-7.4) at room temperature. The probe **NAC** itself exhibited negligible fluorescence corresponding to a peak of weak emission intensity at 450 nm on excitation at 327 nm having low fluorescence quantum yield (Φ_0 = 0.016). Upon addition of N_2H_4 to the receptor solution, a blue-shifted emission peak at 420 nm ($\Delta\lambda$ = 30 nm) was observed and the peak intensity enhanced dramatically at 420 nm in a dose-dependent manner (Fig. 1).

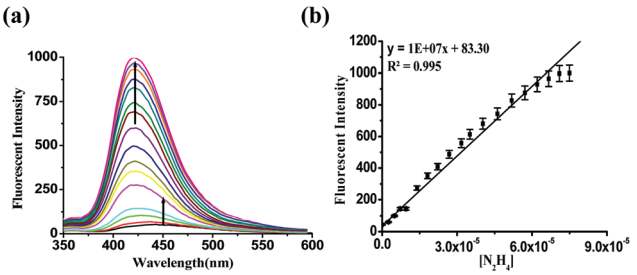

Fig. 1 (a) Fluorescence spectra of the receptor **NAC** (c = 2 × 10^{-5} M) with N_2H_4 (c = 2 × 10^{-4} M) in CH_3CN : HEPES buffer solution (50 : 50, v : v) at pH 7.4. (b) Binding isotherms were recorded at 420 nm with the change of concentration of N_2H_4 including error bars (error amount, 5%, *Y* error bar for both [±] deviation).

The increase of twenty-fold fluorescence intensity causes forty-eight fold enhancement of quantum yield (Φ = 0.774). Actually, this large increase in fluorescence intensity results in the '*naked eye*' blue emission of the resulting solution. The fluorescence intensity at 420 nm of **NAC** also showed a good linearity as a function of the concentration of N_2H_4 in the range of 0 to 85 μM (0–1.5 equiv., linearly dependent coefficient: R^2 = 0.995) (Fig. 1b). From the fluorescence titration experiments, the detection limit of **NAC** for N_2H_4 is determined to be 4.5 μM (0.22 ppb) which is much lower than that of TLV (10 ppb) recommended by EPA and WHO (Fig. S1†). This lower detection limit together with the large fluorescence enhancement and also the increase of quantum yield demonstrates that **NAC** is highly sensitive and selective to N_2H_4. The changes of fluorescence at different time intervals increase with increase of concentrations of hydrazine (Fig. 2).

By using these optical properties at different time intervals and also the first order rate equation, the reaction rate between **NAC** with N_2H_4 was calculated from the time *vs.* fluorescence intensity plot (Fig. S5†) at a fixed wavelength of 420 nm and the rate constant is found to be 1.15 × 10^{-2} s^{-1}. To evaluate the specific nature of **NAC** towards N_2H_4, the influences of other typically encountered anions including F^-, AcO^-, Cl^-, Br^-, I^-, $C_6H_5COO^-$, ATP, DHP, NO_3^-, NO_2^-, SO_3^{2-},

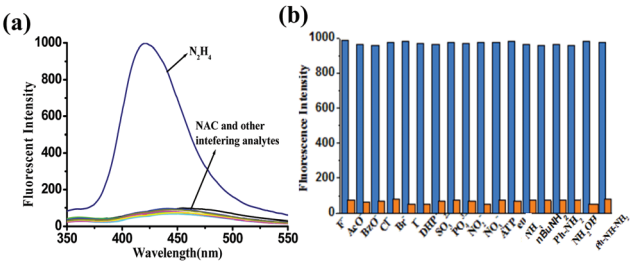

Fig. 2 (a) Fluorescence spectra of the receptor **NAC** (c = 2 × 10^{-5} M) with N_2H_4 and other interfering analytes (c = 2 × 10^{-4} M) in CH_3CN : HEPES buffer solution (50 : 50, v : v) at pH 7.4. (b) Hydrazine selectivity profile of the sensor **NAC** (20 μM): (orange bars) change of emission intensity of **NAC** + 5.0 equiv. of different anions and amines; (blue bars) change of emission intensity of **NAC** + 5.0 equiv. of different anions and amines, followed by 3.0 equiv. N_2H_4 at 420 nm.

PO_4^{3-} as their tetrabutylammonium salts and butylamine, ethylene diamine (en), NH_3, Ph-NH_2, Ph-NH-NH_2, NH_2OH were examined. But, it was observed that within this family of anions and amines, N_2H_4 is the only one that significantly causes cleavage of the chromenyl ring of **NAC** followed by the formation of 3,5-dimethyl-4-methylene-4*H*-pyrazole ring formation in the 2-hydroxynaphthalene backbone. From the competition experiment, it was revealed that N_2H_4 induced fluorescence enhancement remains unperturbed to the coexistence of other interfering analytes and they also become inert towards sensing of hydrazine. So, the probe **NAC** can be utilized to detect N_2H_4 with good selectivity and sensitivity even with the involvement of other relevant species. 2-Hydroxy-1-naphthaldehyde dye is one of the most widely used fluorophores for the development of different fluorescent probes due to its donor as well as an acceptor site. In this fluorophore the –OH moiety in the 2-position acts as a donor site and the aldehyde group in the 1-position acts as an acceptor site. Thus, some degree of intramolecular charge transfer (ICT) process within the naphthalene ring from the 2-position hydroxyl group to the 3-position aldehyde group contributes to its weak yellow fluorescence. Increase in the electron withdrawing properties by the derivatisation of the aldehyde group increases the ICT process to a greater extent from the –OH group and these derivatives have been widely used as receptors in the sensing field.[15] But in our receptor **NAC**, the inhibition of the ICT process occurs by masking of the –OH group in the hemiketal form and thus results in quenching of fluorescence in the **NAC**.

The probable binding mode in the solution phase for **NAC** with N_2H_4 can be explained by a quite different approach (Scheme 3).

Indeed, **NAC** contains two highly reactive sites: one keto-methyl ($-COCH_3$) and another a hemiketal link. This is probably why when N_2H_4 was added to the **NAC** solution, first it (one $-NH_2$ site) reacts with the keto group *via* imine formation (of the keto-methyl group) followed by the cleavage of the hemi-ketal link (by the other $-NH_2$ site). This results in the opening of the chromenyl derivative to make free the –OH group which follows the formation of a pyrazole moiety.

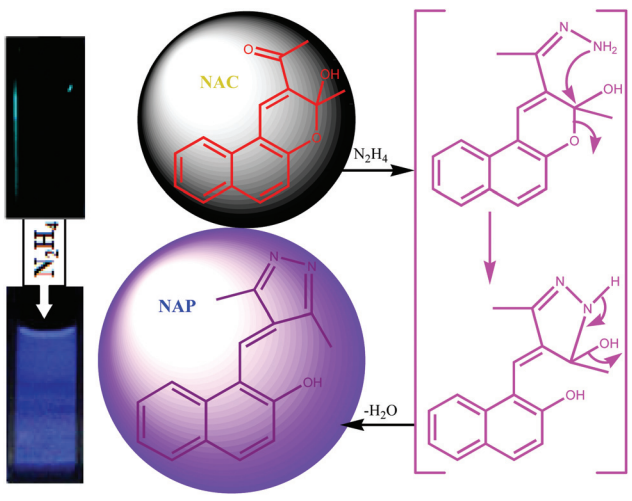

Scheme 3 A plausible mechanism of hydrazinolysis of **NAC** to produce **NAP** (**NAC** + N_2H_4).

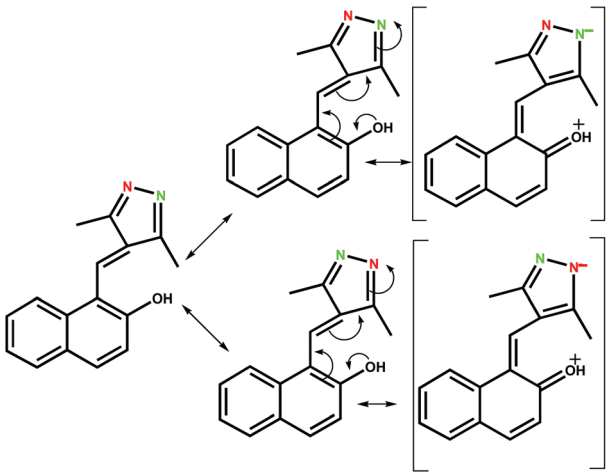

Fig. 3 Strong ICT *via* the high conjugation with the two pyrazole nitrogens (red and blue colored nitrogens indicate the two different nitrogens of the pyrazole ring).

The resulting –OH group in **NAP** (**NAC** + N_2H_4) suffers from a strong ICT due to its large conjugation with the two pyrazole nitrogens and also the basicity of hydrazine (push–pull pathway) (Fig. 3). This increase of ICT causes the appearance of the naked eye blue color in the emission spectra. The binding behavior of N_2H_4 with **NAC** can be explained by comparing the ^{1}H NMR spectra of **NAC**, with its hydrazine adduct **NAP**. By comparing the two spectra it has been shown that on addition of hydrazine to **NAC**, the H_a proton at δ 5.20 ppm (of tertiary –OH) completely disappears and the H_b proton signal (of naphthyl-OH) appears at δ 12.02 ppm by the opening of the chromenyl ring.

On the other hand, the olefinic H_c proton in **NAC** at δ 8.13 ppm shifts to a lower δ value at 6.21 ppm due to paramagnetic shielding for the formation of the pyrazole ring in **NAP**. Furthermore, the other aromatic protons are slightly shielded giving a lower δ value in **NAP** with respect to **NAC** (Fig. 4). The resulting adduct **NAP** (**NAC** + N_2H_4) was also well characterized by ^{1}H NMR, HRMS and ^{13}C NMR spectroscopy. Furthermore the dipstick method is very much useful for the instant qualitative information without using any time consuming instrumental analysis.

In this method, the emission color change in the test strips was identified by immersing the TLC plate in the **NAC** solution followed by evaporating the solvent to dryness, and immersing the plate in an N_2H_4 solution. The emission color change was observed on the plate from colorless to blue upon addition of hydrazine (Fig. 5b). As hydrazine is a so-called carcinogen, its detection in aqueous samples is of very much significance. **NAC** was subjected to hydrazine detection in two pure water samples. The concentrations of hydrazine obtained by our method were found to be in good agreement and consistent with the amounts of added hydrazine (Fig. 5a, Table S1†)

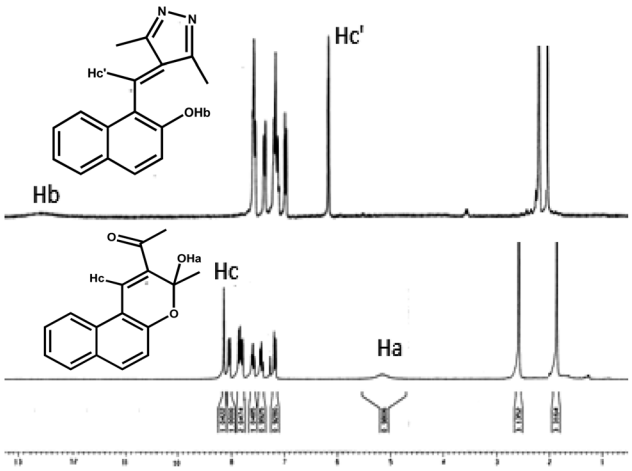

Fig. 4 Partial ^{1}H NMR spectra of the receptor **NAC** with its N_2H_4 adduct (**NAP**) in $CDCl_3$.

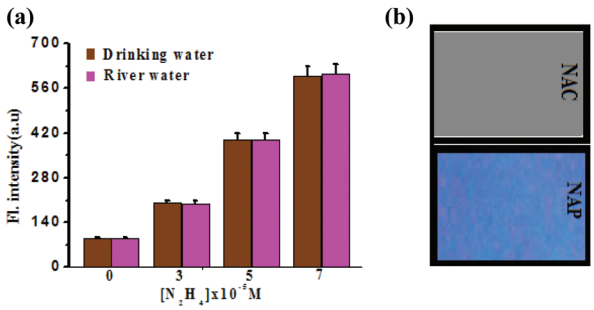

Fig. 5 (a) Fluorescence detection of hydrazine in drinking water and river water by **NAC**. [**NAC**] = 2.0 × 10^{-5} M, [hydrazine] = addition of (0, 30, 50, 70) μM at pH 7.4 in $CH_3CN:H_2O$ (50 : 50, v/v). λ_{ex}(em) = 420 nm. (b) Visualized emission color changes in test strips (solid phase) by immersing TLC sticks into **NAC** and its treatment with hydrazine (c = 2.0 × 10^{-4} M).

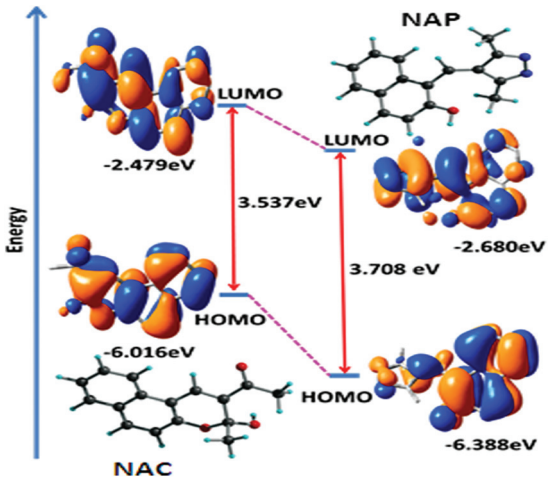

Fig. 6 Energy diagrams of HOMO and LUMO orbitals of **NAC** and **NAP** calculated at the DFT level using a B3LYP/6-311+g** basis set.

which shows that **NAC** qualifies to detect hydrazine in pure water samples quantitatively. The influence of pH for the appearance of fluorescence on the probe **NAC** for the detection of N_2H_4 was also investigated. The **NAC** itself displayed almost no such fluorescence over a wide pH range of 2.0–13.0 (Fig. S7†). However, upon introduction of N_2H_4, an obvious fluorescence enhancement at 420 nm was observed with pH values ranging from 5.1 to 13.0. Thus, the receptor **NAC** showed pH-dependence in the detection of hydrazine and it can function well at physiological pH values.

To ascertain the relationship between structural changes of **NAC** and **NAP** and the optical properties of both the ligands, we employed density functional theory (DFT) and time-dependent density functional theory (TDDFT) calculations with the B3LYP/6-311+g** method using the Gaussian 05 program.

The highest occupied molecular orbital (HOMO) and the lowest unoccupied molecular orbital (LUMO) of **NAC** and **NAP** along with their optimized geometry are shown in Fig. 6. The absorption spectral properties in acetonitrile media were calculated using the TDDFT approach associated with the conductor-like polarizable continuum model (CPCM). Calculated absorption peaks are unequivocally well reasonable with experimentally observed peaks. Some important molecular orbitals involved in the UV-vis transition are shown in Fig. S15 and S16† for **NAC** and **NAP**, respectively. In the case of **NAC** at the ground state, calculated absorption spectra are observed at 378 nm and 333 nm due to the transitions from $S_0 \rightarrow S_5$ and $S_0 \rightarrow S_7$ and for the **NAP**, the two absorption bands (369 nm and 313 nm) can be assigned to the transitions $S_0 \rightarrow S_{10}$ and $S_0 \rightarrow S_{13}$, mainly contributed to the two experimental absorption bands at 372 and 327 nm. The absorption energies along with their oscillator strengths, the main configurations and their assignments are given in Tables S2 and S3†, respectively.

Cell imaging

Human lung cancer cells (NCI-H460) were taken in 6-well plates for detecting fluorescence of **NAC** with hydrazine. Cells were cultured in RPMI 1640 media supplemented with 10% fetal bovine serum (FBS), and 1% antibiotic. Cultured cells were incubated at 37 °C, 5% CO_2 and 95% relative humidity. The stock solution of the **NAC** was prepared in DMSO. As shown in Fig. 7, in controlled incubation of the cells with **NAC**, there is no observable fluorescence but the cell showed intense blue fluorescence in the blue channel when the cells were treated with N_2H_4 followed by the addition of **NAC**. In order to determine the effectiveness of **NAC** and **NAP** (NAC + N_2H_4) towards the human lung cancer cells, the MTT assay[16] was performed (Fig. S2†). As shown in the figure, the survival rate of the cells on treatment with **NAC** is maximum. But when the **NAP** is formed after the addition of hydrazine in the cell, the survival rate gradually decreases giving blue fluorescence. Thus the hydrazine adduct **NAP** is more active and useful for destroying human lung cancer cells.

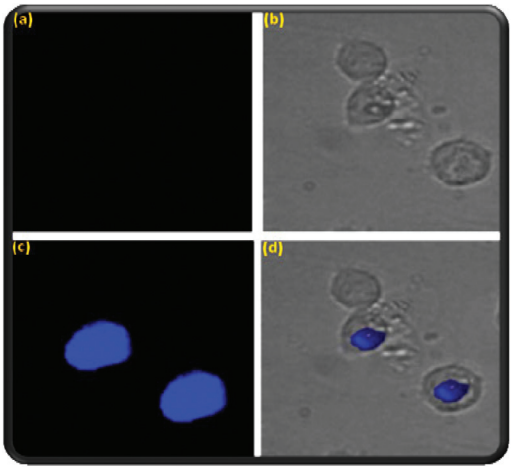

Fig. 7 Fluorescence images of NCI-H460 (a) in the presence of **NAC** ($c = 2 \times 10^{-5}$ M) (dark field image). (b) **NAC** and hydrazine ($c = 6 \times 10^{-2}$ M). The corresponding bright field image in (b), dark field image in (c) & (d) Merged images of (b) and (c).

Conclusions

In conclusion, the distinctive and unique detection of hydrazine by naphthol based chromenyl derivative through the opening of the chromenyl ring *via* the pyrazole ring formation has been well demonstrated here. This new heterocyclic ring formation by hydrazine induced a chemodosimetric approach resulting in the formation of naked eye blue fluorescence. The theoretical study and the spectroscopic characterization of both the **NAC** and **NAP** support excellently the binding phenomenon. It also opens a new approach for hydrazine detection in a condensed system. For the bio-activity test, both **NAC** and **NAP** are highly effective to the human lung cancer cells (NCI-H460). The quick appearance of blue fluorescence for **NAP** on recognition of hydrazine resulting in covalent incorporation and its usefulness for the relatively higher killing rate, compared to **NAC** alone, of the human lung cancer cells (MTT assay) has been documented here.

Experimental section

General

Unless otherwise mentioned, chemicals and solvents were purchased from Sigma-Aldrich Chemicals Private Limited and were used without further purification. Melting points were determined on hot-plate melting point apparatus in an open-mouth capillary and are uncorrected. ^{1}H-NMR spectra were recorded on a Bruker 300 MHz instrument. For NMR spectra, $CDCl_3$ was used as a solvent with TMS as an internal standard. Chemical shifts are expressed in δ units and 1H–1H and 1H–C coupling constants in Hz. UV-vis titration experiments were performed on a JASCO UV-V530 spectrophotometer and the fluorescence experiment was performed using a PerkinElmer LS 55 fluorescence spectrophotometer with a fluorescence cell of 10 mm path.

General methods of UV-vis and fluorescence titration

By the UV-vis method. For UV-vis titrations, a stock solution of the sensor was prepared ($c = 2 \times 10^{-5}$ M) in CH_3CN : HEPES buffer solution (v : v, 50 : 50) at pH 7.4. Solutions of various concentrations containing the sensor and increasing concentrations of hydrazine were prepared separately. The spectra of these solutions were recorded by means of UV-vis methods.

By the fluorescence method. For fluorescence titrations, a stock solution of the sensor ($c = 2 \times 10^{-5}$ M) was prepared for the titration of cations in CH_3CN : HEPES buffer solution (v : v, 50 : 50) at pH 7.4. The solution of the guest anions like F^-, AcO^-, Cl^-, Br^-, I^-, $C_6H_5COO^-$, ATP, DHP, NO_3^-, NO_2^-, SO_3^{2-}, PO_4^{3-} as their tetrabutylammonium salts and butylamine, ethylene diamine(en), NH_3, Ph-NH_2, Ph-NH-NH_2, NH_2OH were also prepared in the order $c = 2 \times 10^{-4}$ M. Solutions of various concentrations containing the sensor and increasing concentrations of different ions were prepared separately. The spectra of these solutions were recorded by means of fluorescence methods.

Determination of the fluorescence quantum yield. Here, the quantum yield φ was measured using the following equation:

$$\varphi_x = \varphi_s(F_x/F_s)(A_s/A_x)(n_x^2/n_s^2)$$

where X and S indicate the unknown and standard solution, respectively, φ = quantum yield, F = area under the emission curve, A = absorbance at the excitation wave length, n = index of refraction of the solvent. Here φ measurements were performed using anthracene in ethanol as the standard [$\varphi = 0.27$] (error ~10%).

Methods for the preparation of the receptor NAC and its hydrazine adduct NAP

Synthesis of 2-hydroxy-1-naphthylaldehyde. 2-Hydroxy-1-naphthylaldehyde was synthesized by the reported procedure.[17] β-Naphthol (1 g, 0.0069 mol) was placed in a 100 ml r.b. flask fitted with a reflux condenser, a magnetic stirrer and a dropping funnel. It was then dissolved in EtOH at 80–90 °C. NaOH (2 g, 0.05 mol) in 20 mL water was then added dropwise to this hot solution till the solution became darker. After half an hour, $CHCl_3$ (1.3 g, 0.011 mol) was added dropwise using the dropping funnel. Development of deep blue coloration indicated that the reaction has started. At the end point of the addition, the sodium salt of phenolic aldehyde was separated out. The reaction mixture was stirred for six hours. Excess ethanol and chloroform were distilled off. The dark oil left was mixed with a considerable amount of sodium chloride. Sufficient water was added to dissolve the salt, and the oil was separated and washed with hot water. Then, the solution was neutralized with dilute hydrochloric acid and extracted with chloroform. Finally, the product was purified by 60–120 silica gel using 1–2% ethyl acetate in pet ether. Yield of the product was 500 mg (50%). Melting point: 79–80 °C.

Synthesis of NAC [1-(3-hydroxy-3-methyl-3*H*-benzo[*f*]-chromen-2-yl) ethanone]. **NAC** was synthesized by the following procedure. 2-Hydroxy-1-naphthylaldehyde (500 mg,

2.90 mmol), acetyl acetone (300 mg, 2.99 mmol), and 1 mL of piperidine were dissolved in 30 mL of absolute dry ethanol. After the solution was stirred at room temperature for 2 h, an orange precipitate was separated out. The orange solid was filtered and collected, and the product was crystallized from absolute ethanol to afford the compound **NAC** (yield: 500 mg, 67%).

Mp. 110–120 °C. ^{1}H NMR ($CDCl_3$, 300 MHz): δ (ppm): 8.13 (s, 1H), 8.04 (d, J = 9 Hz, 1H), 7.82 (q, J = 13.5 Hz, 2H), 7.58 (q, J = 9 Hz, 1H), 7.42 (t, J = 7.5 Hz, 1H), 7.16 (d, J = 9 Hz, 1H), 5.15 (s, 1H), 2.57 (s, 3H), 1.85 (s, 3H). **^{13}C NMR ($CDCl_3$, 75 MHz): δ (ppm):** 198.25, 152.78, 134.04, 130.77, 130.61, 130.35, 129.28, 129.02, 127.89, 124.49, 120.58, 118.10, 111.55, 99.49, 27.51, 26.42. **HRMS (ESI-TOF): (m/z, %):** $[M + Na]^+$ calcd for $C_{16}H_{14}O_3Na$ is 277.0841; Found: 277.0536; **Elemental analysis**: Calcd value: C, 75.57; H, 5.55; Observed value: C, 75.53; H, 5.59.

Synthesis of the receptor NAC + N_2H_4 adduct (NAP). NAC (300 mg, 1.18 mmol) was added to acetonitrile (20mL) and stirred at room temperature to dissolve it to form a solution. After sometime, hydrazine hydrate (60 mg, 1.18 mmol) was added to it. The mixture was stirred for 10 minutes and after checking the completion of the reaction by TLC, the crude product was purified by silica gel column chromatography using 20% ethylacetate in pet-ether (v/v) to give a white compound **NAP** (150 mg, 50%).

Mp. 150–160 °C. **^{1}H NMR ($CDCl_3$, 300 MHz): δ (ppm):** 11.88 (s, 1H), 7.81(d, J = 9 Hz, 1H), 7.68 (t, J = 9.0 Hz, 1H), 7.44 (m, 1H), 7.22 (m, 2H), 7.06 (q, J = 7.5 Hz, 1H), 6.21 (s, 1H), 2.02 (s, 3H), 1.87 (s, 3H). **^{13}C NMR ($CDCl_3$, 75 MHz): δ (ppm):** 155.81, 155.53, 132.29, 129.56, 128.82, 128.59, 126.31, 122.51, 121.71, 119.81, 113.97, 112.90, 57.50, 25.36, 16.61, 10.98. **HRMS (ESI-TOF):** (m/z, %): $[M + H]^+$ calcd for $C_{16}H_{14}N_2O$ is 251.1184; Found: 251.1182; **Elemental analysis:** calcd value: C, 76.78; H, 5.64; N, 11.19. Observed value: C, 76.82; H, 5.62; N, 11.17.

Acknowledgements

The authors thank the DST and CSIR (Govt. of India) for financial support. A.K.D. and acknowledge the CSIR for providing fellowships.

Notes and references

1 E. L. Que, D. W. Domaille and C. J. Chang, *Chem. Rev.*, 2008, **108**, 1517.
2 A. Louie, *Chem. Rev.*, 2010, **110**, 3146.
3 M. E. Jun, B. Roy and K. H. Ahn, *Chem. Commun.*, 2011, **47**, 7583.
4 J. Du, M. Hu, J. Fan and X. Peng, *Chem. Soc. Rev.*, 2012, **41**, 4511.
5 Y. Yang, Q. Zhao, W. Feng and F. Li, *Chem. Rev.*, 2012, **113**, 192.
6 (*a*) J. Liu, Y. Li, J. Jiang and X. Huang, *Dalton Trans.*, 2010, **39**, 8693; (*b*) Z. Zhao, G. Zhang, Y. Gao, X. Yang and Y. Li, *Chem. Commun.*, 2011, **47**, 12816; (*c*) X. Chen, Y. Xiang, Z. Li and A. Tong, *Anal. Chim. Acta*, 2008, **625**, 41.
7 (*a*) U. Ragnarsson, *Chem. Soc. Rev.*, 2001, **30**, 205; (*b*) S. S. Narayanan and F. Scholz, *Electroanalysis*, 1999, **11**, 465; (*c*) K. Yamada, K. Yasuda, N. Fujiwara, Z. Siroma, H. Tanaka, Y. Miyazaki and T. Kobayashi, *Electrochem. Commun.*, 2003, **5**, 892; (*d*) J. Wang and L. Chen, *Anal. Chem.*, 1995, **67**, 3824.
8 (*a*) S. Virji, R. B. Kaner and B. H. Weiller, *Chem. Mater.*, 2005, **17**, 1256; (*b*) G. Wang, C. Zhang, X. He, Z. Li, X. Zhang, L. Wang and B. Fang, *Electrochim. Acta*, 2010, **55**, 7204; (*c*) H. Yang, B. Lu, L. Guo and B. Qi, *J. Electroanal. Chem.*, 2011, **650**, 171; (*d*) S. J. Richard Prabakar and S. J. Sriman Narayanan, *Electroanal. Chem.*, 2008, **617**, 111.
9 (*a*) S. Garrod, M. E. Bollard, A. W. Nicholls, S. C. Connor, J. Connelly, J. K. Nicholson and E. Holmes, *Chem. Res. Toxicol.*, 2005, **18**, 115; (*b*) C. A. Reilly, *Chem. Res. Toxicol.*, 1997, **10**, 328.
10 S. W. Thomas and T. M. Swager, *Adv. Mater.*, 2006, **18**, 1047.
11 (*a*) M. G. Choi, J. Hwang, J. O. Moon, J. Sung and S. K. Chang, *Org. Lett.*, 2011, **13**, 5260; (*b*) M. G. Choi, J. O. Moon, J. Bae, J. W. Lee and S. K. Chang, *Org. Biomol. Chem.*, 2013, **11**, 2961; (*c*) L. M. Hee, B. Yoon, J. S. Kim and J. L. Sessler, *Chem. Sci.*, 2013, **4**, 4121.
12 J. Fan, W. Sun, M. Hu, J. Cao, G. Cheng, H. Dong, K. Song, Y. Liu, S. Sun and X. Peng, *Chem. Commun.*, 2012, **48**, 8117.
13 X. Chen, Y. Xiang, Z. Li and A. Tong, *Anal. Chim. Acta*, 2008, **625**, 41.
14 (*a*) D. P. Roek, J. E. Chateauneufm and J. F. Brennecke, *Ind. Eng. Chem. Res.*, 2000, **39**, 3090; (*b*) Z. X. Li, L. F. Zhang, X. Y. Li, Y. K. Guo, Z. H. Ni and J. H. Chen, *Dyes Pigm.*, 2012, **94**, 606; (*c*) M. Ali, M. Jha, S. K. Das and S. K. Saha, *J. Phys. Chem. B*, 2009, **113**, 15563.
15 (*a*) S. Goswami, A. K. Das, D. Sen, K. Aich, H. K. Fun and C. K. Quah, *Tetrahedron Lett.*, 2012, **53**, 4819; (*b*) S. Goswami, A. K. Das, K. Aich and A. Manna, *Tetrahedron Lett.*, 2013, **54**, 4215; (*c*) S. Goswami, S. Maity, A. K. Das, A. C. Maity, T. K. Mandal and S. Samanta, *Tetrahedron Lett.*, 2013, **54**, 5232; (*d*) S. Goswami, S. Maity, A. K. Das and A. C. Maity, *Tetrahedron Lett.*, 2013, **54**, 6631.
16 A. Roy, K. Khanra, A. Mishra and N. Bhattacharyya, *Int. J. Adv. Res.*, 2013, **1**, 193.
17 (*a*) Fosse, *Bull. Soc. Chim. Fr.*, 1901, **25**, 373; (*b*) Kolesnikov, Korshak and Krakovnaya, *Zh. Obshch. Khim.*, 1951, **21**, 397 [C.A., 45, 7553 (1951)].

